The Bight Basin, Evolution & Prospectivity III; FE modelling

Rebecca Farrington
School of Earth Sciences
University of Melbourne
Rebecca.Farrington@unimelb.edu.au

Kevin C Hill
School of Earth Sciences
University of Melbourne
Kevin.Hill@unimelb.edu.au

Jane Cunneen
School of Earth and Planetary Sciences
Curtin University
Jane.Cunneen@curtin.edu.au

Romain Beucher
School of Earth Sciences
University of Melbourne
Romain.Beucher@unimelb.edu.au

Louis Moresi
School of Earth Sciences
University of Melbourne
Louis.Moresi@unimelb.edu.au

SUMMARY

This paper outlines a Finite Element modelling workflow using the software package 'Underworld' that is applied to sedimentary basin undergoing multiple rifting events. The evolution of the resulting strain rate, viscosity structure, temperature field, and sedimentary structures can be tracked. Application to the Ceduna Sub-basin is discussed.

Key words: Ceduna, modelling extension, modelling sedimentation, finite element modelling, geodynamics.

INTRODUCTION

The Bight Basin was formed during a failed rifting event during the break up of East Gondwana between the Jurassic to Lower Cretaceous. This period of mechanical extension was followed by a period of very slow, or non-existent, extension as evidenced by thermal subsidence (Hill et al., This Volume). A second period of slow spreading commenced during the Turonian breakup (95 Ma to 85 Ma) of the Australian and Antarctic continents. Throughout both the extension and thermal subsidence phases, the Ceduna delta was active, depositing numerous sedimentary layers within the Bight Basin.

The aim of this study is to understand the tectonic and thermal evolution of the Bight Basin given its multiple extensional periods and extensive sedimentary record. This was achieved by interrogating a number of conceptual models of rift basins and further developing the finite element modelling of multiphasic rifting published by Salerno et. al. (2014). In this work a variety of rift basins were produced by imposing two rifting events with an intermediate cooling phase, defined by recovery of the steady state geotherm within the rifted lithosphere and asthenosphere. The only varying parameter within this study was the extensional velocity of the rifting events, all other rheological and geometrical parameters were held constant. Of particular interest to the current study of the Ceduna Sub-basin is the results from the slow-slow model, model r1-r2 outlined in Figure 3(b) of Salerno et al (2014), shown in Figure 1. Neglecting the sediment deposits within the modern Ceduna sub-Basin, the similarities between the finite element model and the Bight Basin is striking, with the model corresponding to the magnitude and wavelength of crustal deformation within Ceduna. However, without modelling the sediment loading, an important contributor in the evolution of the Ceduna Sub-basin remains unaccounted.

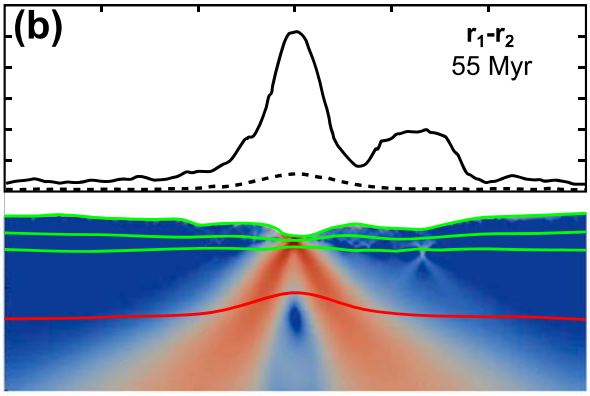

Figure 1. A reproduction of Salerno et al. Figure 3(b) showing (top) the crustal and lithospheric (dashed) thinning factors and (bottom) the strain rate map with material (green) and Lithosphere Asthenosphere Boundary (red).

This study aims to include the additional mechanical and thermal effects of sedimentary deposition into a generalised model of two-phase regional scale rifting system. Additionally, this study shows the ability of the Underworld software package to model complex thermomechanical rifting environments, including complex rheological behaviour, realistic boundary conditions (variable extensional velocities, free-surface and isostatic base), and sediment deposition. Application to the Ceduna Sub-basin shows promising results for understanding the primary drivers of the thermomechanical evolution of the rifted southern margin of Australia.

METHOD

Using the Geodynamics software package Underworld (Moresi, 2007 and Moresi, 2018) a model workflow has been developed to study the interaction of multiple rifting events with time dependent sedimentation. The initial model set up is modified from Tutorial 1, a thermomechanical lithospheric model of extension, from Beucher et al., (2019).

Underworld is an open-source, particle-in-cell finite element fluid dynamics code tuned for large-scale geodynamics simulations, solving Stokes flow within the infinite Prandtl number approximation. The formation of a sedimentary basin can be modelled by prescribing material properties of the upper crust, lower crust, lithospheric mantle and mantle, within a domain with initial and boundary temperature conditions consistent with far field (large scale) tectonic plate velocities. This material domain is then deformed given the prescribed thermal and rheological behaviour under an extensional velocity in the direction normal to vertical.

In this study all material variables are held constant for all models. The initial material layout with the model domain is shown in Figure 2. The upper crust (UC), lower crust (LC) and mantle (M) are defined using a number of experimental study parameterisations of a viscous creep rheology, defined as

$$\eta = 0.5\, A^{-1/n}\, \dot{\epsilon}^{(1-n)/n} \exp\left(\frac{E + PV}{nRT}\right)$$

With η viscosity, A an experimentally determined prefactor, $\dot{\epsilon}$ strain rate, n stress exponent, E activation energy, P pressure, V activation volume, R gas constant and T temperature. We have assumed the strain rate is grain size independent. The upper crust and sediment (S) defined using the parameters of Wet Quartz Dislocation from Gleason and Tullis (1995), the lower crust Dry Columbia Diabase Dislocation from Mackwell et. al. (1998), and the lithospheric mantle (LM) and mantle defined using Dry Olivine Dislocation from Karato and Wu (1990). A free surface at the upper boundary of the solid Earth is modelled using a Sticky Air and Air layer with a linear viscosity of 10^{19} Pa.s and 10^{20} Pa.s respectively. Yielding is implemented using the crustal parameters outlined in Husimans et. al. (2011).

The density of the solid Earth material is defined by a reference density (S 2,300 kg/m^3, UC 2,700 kg/m^3, LC 2,900 kg/m^3, LM and M 3,370 kg/m^3), and corresponding thermal expansivity of $3x10^{-5}K^{-1}$.

The initial temperature is prescribed using a steady state solution with constant boundary conditions of 20ºC and 1330ºC along the top and bottom wall respectively. The thermal diffusivity and capacity of the solid Earth material were 10^{-6} m^2/s and 1kJ/K.kg, with the air and sticky air having significantly less thermal capacity, at 100 J/K.kg. Radiogenic heat production was prescribed of 0.6mW/m^3 for sediment, 0.7mW/m^3 for upper and lower crust, and 0.02mW/m^3 for the lithospheric mantle.

Extensional velocity (Dirichlet) boundary conditions were applied to the vertical (right/left) walls. Isostasy modelled using stress (Neumann) boundary conditions along the horizontal (top/bottom) walls. Plastic strain was initialised using a random gaussian distribution of damaged focused at a depth of 35km. The models presented within this study have a spatial resolution of 500m. Sedimentation was included by transforming 'air' and 'sticky-air' to 'sediment' material at a defined elevation of .

The only model variables considered in this study was the inclusion of sedimentation (including timing and location), the extension velocity of rifting events, and during of cooling periods.

RESULTS

Using the geodynamic code Underworld (Moresi et al., 2007; Moresi et al., 2018), we modelled the deformation resulting from multiple rifting events with or without sedimentation. The numerical models explore a parameterised rifting plate boundary. Outlined below are the results of two models with the same rifting rate (i) without and (ii) with sedimentation included from time = 2.8ma.

Figure 3 below shows the Finite Element Underworld model outcome after 2.8ma of rifting at a rate of 2.5cm/yr. The strain rate colour map can be seen to localise within a number of shear zones resulting in a basin of approximately 100km width. A single shear zone cuts through the entire lithosphere, with a number of additional shear zones of similar strain rate of crustal scale in length.

Figure 4 shows the same model after further extension at time 4.0ma. The crust has been hyper thinned, with the mantle exposed in a wide basin encompassing a secondary deposition zone at a distance from the active spreading centre.

Figure 5 shows the results of a model that included sedimentation from a time of 2.8ma (Figure 2). While no details of the sedimentary structures are shown within this figure, a significant difference between the model shown in Figure 3 can be seen. The viscosity structure in the region of the active shear zones and the sediments can be seen. Additionally, a number of active shear zones were maintained for a longer duration than for the model without sedimentation. Feedback between sedimentation and the shear zones alters the evolution of crustal thinning and shear zones. Figure 6 isolates the sedimentary basin from the larger scale deforming crust and lithosphere, showing the temperature of the sediments at a time of 4ma.

CONCLUSIONS

The general style of time dependent, force driven finite element modelling employed within this study gives a primary understanding of basin evolution. An understanding against which other parameters can be tested, for example subsidence rate, heat flow, sediment distribution, porosity through time. Relatively simple regional models can quickly test concepts to determine likelihood, for example the nature and duration of uplift and erosion events. More complex 3D models can predict and test sediment distribution patterns, burial through time, pulses of uplift and erosion. Both time and space resolution can be modified as needed by the end user.

While these results are for extensional rates at the upper limit of the Ceduna Sub-basin, the models show there is significant interaction between rift events and sedimentation within the actively deforming basin. The Underworld workflow developed for this study is robust and provides many interesting avenues of investigation, of specific interest is the parameterisation of the Ceduna Sub-basin as discussed by Cunneen et al. (This volume) and Hill et al. (This volume).

ACKNOWLEDGMENTS

The authors acknowledge the support of the ARC Research Hub for Basin Geodynamics and Evolution of Sedimentary Systems (Basin GENESIS Hub, ARC IH130200012). RJF was supported under Australian Research Council's Discovery Projects funding scheme (project number DP130101946). This research was undertaken with the assistance of resources and services from the National Computational Infrastructure (NCI), which is supported by the Australian Government.

REFERENCES

Beucher et al., (2019). UWGeodynamics: A teaching and research tool for numerical geodynamic modelling. Journal of Open Source Software, 4(36), 1136, https://doi.org/10.21105/joss.01136

Cunneen J., DePledge C., Lowe S., Hill K.C., Godfrey C., Buckingham A. & Farrington R. This volume. The Bight Basin, Evolution & Prospectivity I; gravity, deep seismic & basin morphology.

Gleason, G. C., & Tullis, J. (1995). A flow law for dislocation creep of quartz aggregates determined with the molten salt cell. Tectonophysics, 247(1-4), 1-23.

Hill, K.C., Cunneen, J.C., & Farrington, R., this volume. The Bight Basin, Evolution & Prospectivity II: Seismic, structure and balanced sections.

Huismans, R., & Beaumont, C. (2011). Depth-dependent extension, two-stage breakup and cratonic underplating at rifted margins. Nature, 473(7345), 74.

Karato, S. I., & Wu, P. (1993). Rheology of the upper mantle: A synthesis. Science, 260(5109), 771-778.

Mackwell, S. J., Zimmerman, M. E., & Kohlstedt, D. L. (1998). High-temperature deformation of dry diabase with application to tectonics on Venus. Journal of Geophysical Research: Solid Earth, 103(B1), 975-984.

Moresi, L., J. A. Mansour, J. Giordani, R. Farrington, & R. Beucher (2018), Underworld 2 (Version 2.5.1b), doi:10.5281/zenodo.1434224.

Moresi, L., Quenette, S., Lemiale, V., Mériaux, C., Appelbe, B. & -B. Mühlhaus, H. (2007) Computational approaches to studying non-linear dynamics of the crust and mantle. Phys. Earth Planet. Inter., 163, 69–82.

Salerno, V. M., F. A. Capitanio, R. J. Farrington, and N. Riel (2016), The role of long-term rifting history on modes of continental lithosphere extension, J. Geophys. Res. Solid Earth, 121, doi:10.1002/2016JB013005.

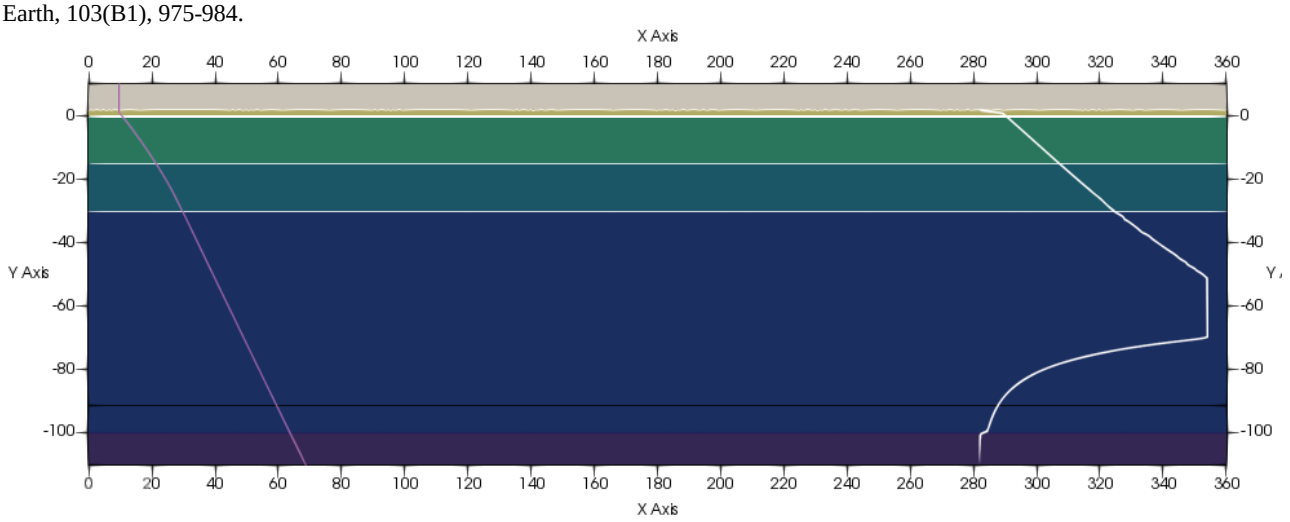

Figure 1. Initial material layout (colour map and horizontal white lines, top to bottom) air, sticky air, upper crust, lower crust, lithospheric mantle and mantle within the model domain of 0km < x < 360km, -110km < y <10 km. The 1400ºK Lithosphere-Asthenospheric Boundary (LAB, horizontal black line), temperature profile with depth (purple, top=293.15ºK, bottom=1603.15ºK) and initial viscosity (η) profile for a strain rate of 10^{-15} s^{-1} (white, 10^{18} Pa.s < η < 10^{23} Pa.s).

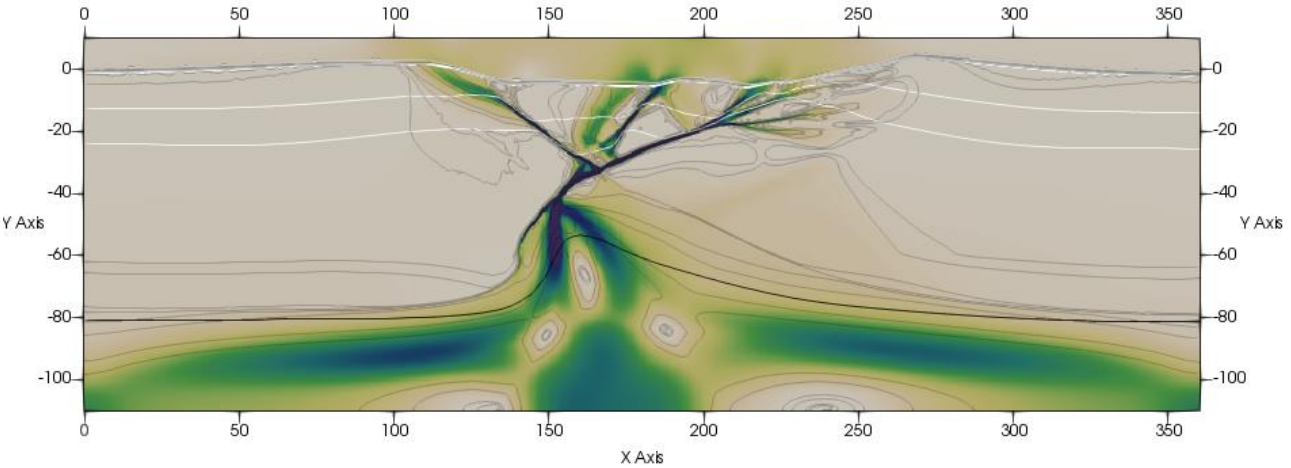

Figure 3. The strain rate (second invariant, colour map) at time = 2.8ma, with the 1400ºK Lithosphere-Asthenospheric Boundary (LAB, line) and viscosity contours (grey lines) of the upper crust, lower crust, lithospheric mantle and mantle (white contours) under an extensional velocity of 2.5 cm/yr after 2.8 ma of extension.

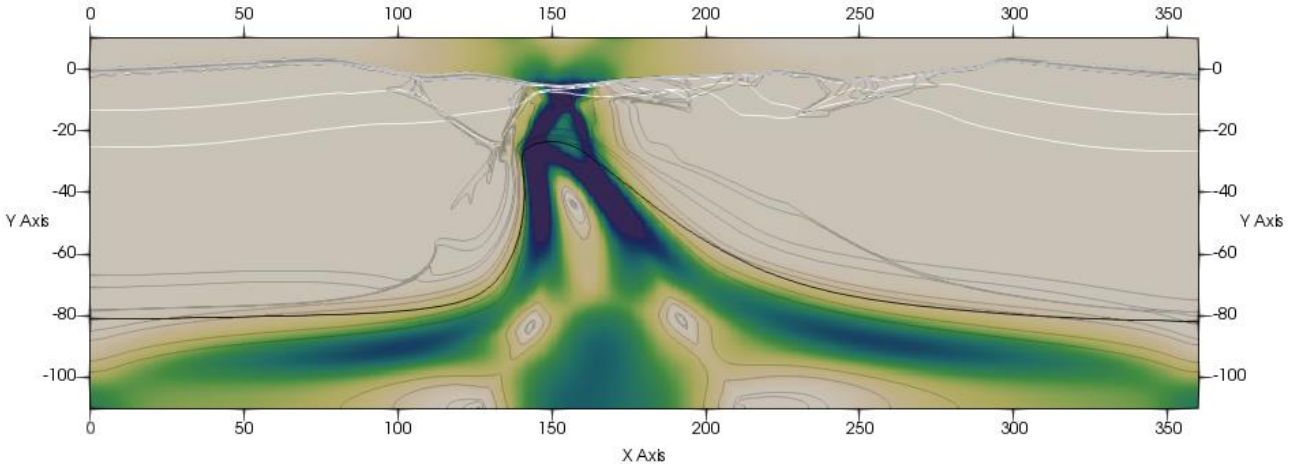

Figure 4. The strain rate after 4.0 ma of extension for model shown in Figure 2.

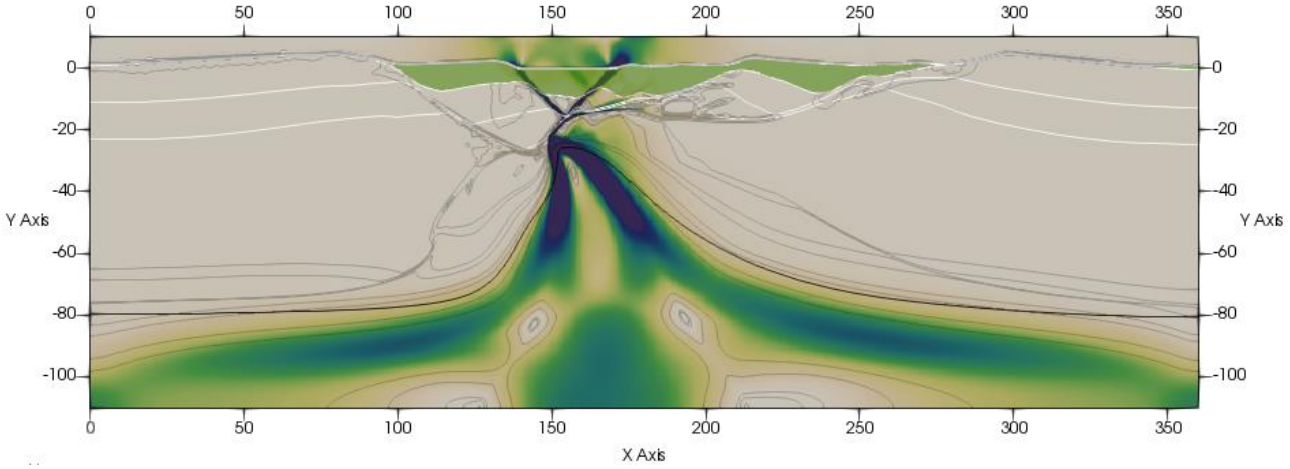

Figure 5. The strain rate at time = 4.0ma for a model with erosion introduced at time = 2.8 ma, colour in green. Viscosity, temperature and material contours as for Figure 2.

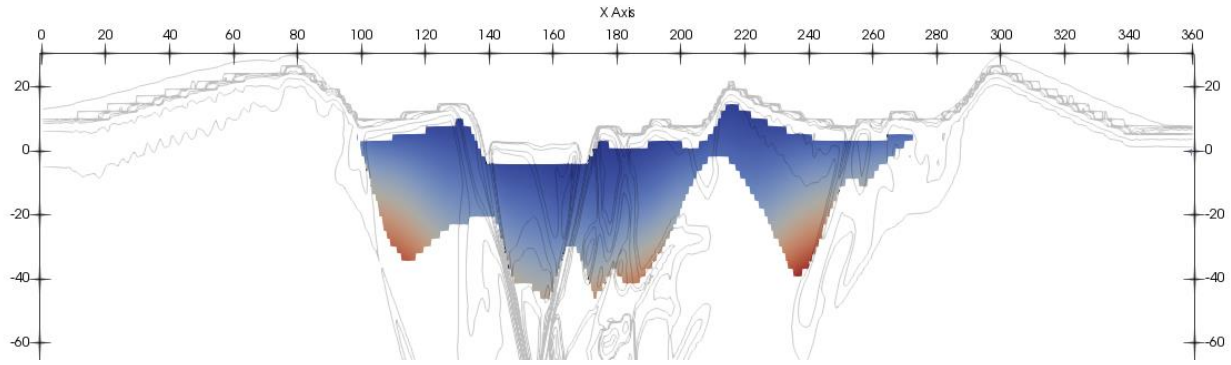

Figure 6. The temperature, 23ºC (blue) to 230ºC (red), within sediments only at time = 4.0ma, for the model shown in Figure 4. Note vertical exaggeration of 1:5, highlighting the 500m scale Finite Element mesh resolution. Viscosity contours as for figures above.